

A New Method to Determine Hydraulic Conductivity and Storage Coefficient through Simultaneous Measurements of Fluid Pressure and Strains

Tomochika Tokunaga^{1)*}, Hiroshi Kameya²⁾, Katsuro Mogi¹⁾ and Rika Aoyagi¹⁾

¹⁾ Department of Geosystem Engineering, University of Tokyo

²⁾ Core Laboratory, OYO Corporation, Omiya, Japan

Abstract

The concept of storage coefficient was discussed based on the theory of poroelasticity. Several different storage coefficients can be defined by different mechanical boundary conditions and assumptions on the physical properties of constitutive materials. The specific storage, which is usually used in the field of hydrogeology, is shown to be defined when the representative elementary volume is maintained in a state of zero lateral strain and constant stress perpendicular to that plane. This means that the specific storage is not measured in most laboratory pore pressure tests because the boundary condition of zero lateral strain is not satisfied. Instead, we measure a three-dimensional storage coefficient.

In the latter sections of this paper, we present a new method to determine both the hydraulic conductivity and the storage coefficient through simultaneous measurements of fluid pressure and strains. In this study, a new endplug with a built-in valve was developed to accurately measure the poroelastic parameters. Our experimental assembly significantly reduces the extra volume of the system and is readily adapted to the various pore-fluid boundary conditions. The three-dimensional storage coefficient was calculated from the volumetric poroelastic parameters obtained from quasi-static strain data, and the hydraulic conductivity from the transient pore pressure diffusion data. Transient strain behavior during the pore pressure diffusion stage was used to self-check the accuracy of the parameters obtained. This technique does not require complicated inversion calculations and can be used easily for parameter identification.

Key words: hydraulic conductivity, storage coefficient, poroelasticity, fluid flow

1. Introduction

Hydraulic conductivity and storage coefficients are two parameters necessary to analyze fluid flow process through porous media. There have been extensive researches and discussions on the hydraulic conductivities of geological materials.

There have been several researches on determining the storage coefficient (specific storage) of the porous medium: one is the transient pulse method (Neuzil *et al.* 1981, Wang and Hart 1993, Zhang *et al.* 2000, Hart and Wang, 2001), and another uses the transient stage of the flow-pump experiments (Olsen

et al. 1988, Esaki *et al.* 1996). According to error estimates of the transient pulse method (Wang and Hart 1993), the storage coefficient is measured much less accurately than hydraulic conductivity. Also, the transient process of the flow-pump experiments is affected by the storage capacity of the equipment (Esaki *et al.* 1996), and it is not a straightforward task to determine the storage coefficient of the porous medium from experimental pore pressure data (Kameya *et al.* 2001).

In this paper, we first review the concept of storage coefficient based on the theory of poroelastic-

*e-mail : tokunaga@geosys.t.u-tokyo.ac.jp (7-3-1 Hongo, Bunkyo-ku, Tokyo 113-8656, Japan)

ity. As will be shown in the following section, an accurate definition of the storage coefficient is given (Green and Wang 1990), in which the coefficient is explained by the elastic properties of a porous medium and the compressibility of pore fluid. Thus, it can be expected that both hydraulic conductivity and storage coefficient are determined by simultaneous measurements of fluid pressure and strains in experiments designed originally to measure the hydraulic conductivity of the medium. In the latter sections of this paper, we present a new method to determine both hydraulic conductivity and storage coefficient directly by measuring both fluid pressure and strains of the porous medium.

2. Poroelastic theory and the storage coefficient

The storage coefficient is defined as the volume of water released from storage under a unit decline of average hydraulic head within the unit volume (Narasimhan and Kanehiro, 1980; Green and Wang, 1990). This definition is expressed mathematically as:

$$S = \frac{1}{\rho_f} \left(\frac{dm_f}{dh} \right) = g \left(\frac{dm_f}{dP} \right) \quad (1)$$

where S is storage coefficient, ρ_f is pore fluid density, m_f is fluid mass per unit bulk volume of porous material, h is hydraulic head, g is gravitational acceleration, and P is pore fluid pressure. Because expansion of the water and compression of the framework both contribute to the released water volume, it is necessary to understand the precise definition of the storage coefficients and to use the coefficient that fits the physical conditions of the problems considered. In this section, we derive several different storage coefficients based on the theory of poroelasticity and show the relationship between these coefficients and mechanical boundary conditions and/or assumptions on the physical properties of constitutive materials.

2.1 The theory of poroelasticity

The theory of poroelasticity was introduced by Biot (1941), and developed in the field of applied mechanics. Recently, this theory has been applied in the field of earth sciences and hydrogeology (Rice and Cleary, 1976; Detournay and Cheng, 1993; Wang, 1993; Wang, 2000). The constitutive equations for linear isotropic poroelastic materials can be written (Rice and Cleary, 1976; Wang, 1993) as:

$$2G\varepsilon_{ij} = \sigma_{ij} - \frac{1}{3} \left(1 - \frac{2G}{3K} \right) \sigma_{kk} \delta_{ij} + \frac{2G}{3} \left(\frac{1}{K} - \frac{1}{K_s} \right) P \delta_{ij} \quad (2)$$

$$m_f = \rho_f \left(\frac{1}{K} - \frac{1}{K_s} \right) \left(\frac{1}{3} \sigma_{kk} + \frac{1}{B} P \right) \quad (3)$$

where G is shear modulus, ε_{ij} is bulk strain tensor of the representative elementary volume (REV) of a porous medium, σ_{ij} is total stress tensor on an REV, K is drained bulk modulus, K_s is unjacketed bulk modulus, δ_{ij} is Kronecker's delta, and B is Skempton's B coefficient. The total stress σ_{ij} is the total force in the i^{th} direction acting per unit area on the face whose normal is in the j^{th} direction. The area is that enclosed by the perimeter of the face and includes both solid grains and pores (Wang, 2000). The sign convention follows that of general elasticity; that is, tensile stresses are positive, extensions are positive for strains, and increases of pore pressure and fluid content are taken as positive. The linear approximation can be considered valid for rocks if strains, stresses, and fluid pressure are considered to be incremental quantities relative to some reference state. Thus, the material constants are anticipated to be functions of the stress and the fluid pressure of the reference state.

Fluid flow in a porous medium is generally considered to follow Darcy's law. Darcy's law is written as:

$$q_i = - \frac{\kappa}{\rho_f g} \frac{\partial P}{\partial x_i} \quad (4)$$

where q_i is specific discharge (fluid volume per unit area per unit time) for i^{th} direction, and κ is hydraulic conductivity. In the case where fluid source/sink does not exist in the system, the conservation of fluid mass is expressed as:

$$\frac{\partial(\rho_f q_i)}{\partial x_i} + \frac{\partial m_f}{\partial t} = 0 \quad (5)$$

Assuming that hydraulic conductivity and fluid density do not change in space, and substituting equations (3) and (4) into (5) yields

$$\begin{aligned} \kappa \nabla^2 P &= \rho_f g \left(\frac{1}{K} - \frac{1}{K_s} \right) \frac{1}{B} \frac{\partial}{\partial t} \left(P + \frac{B}{3} \sigma_{kk} \right) \\ &= \frac{\rho_f g \alpha}{KB} \frac{\partial}{\partial t} \left(P + \frac{B}{3} \sigma_{kk} \right) \end{aligned} \quad (6)$$

where α is Biot-Willis coefficient (Wang, 1993) and is defined as

$$\alpha = 1 - \frac{K}{K_s} = \frac{1}{B} \left(1 - \frac{K}{K_u} \right) \quad (7)$$

where K_u is the undrained bulk modulus. Skemp-

ton's B coefficient can be written (Wang, 1993) as:

$$B = \frac{\frac{1}{K} - \frac{1}{K_s}}{\frac{1}{K} - \frac{1}{K_s} + \phi \left(\frac{1}{K_f} - \frac{1}{K_\phi} \right)} \quad (8)$$

and hence the equation (6) becomes

$$\kappa \nabla^2 P = \rho_f g \left[\frac{1}{K} - \frac{1}{K_s} + \phi \left(\frac{1}{K_f} - \frac{1}{K_\phi} \right) \right] \frac{\partial}{\partial t} \left(P + \frac{B}{3} \sigma_{kk} \right) \quad (9)$$

where ϕ is porosity, K_f is bulk modulus of pore fluid, and K_ϕ is reciprocal of the unjacketed pore compressibility. When the solid phase of the porous material is composed of a single constituent, K_ϕ is equal to K_s (Berryman, 1992). Equation (9) is the general form of the governing equation for fluid flow. This equation suggests that, in general, the fluid flow process is coupled with the deformation of a porous material, because mean normal stress ($1/3 \sigma_{kk}$) appears in the equation.

The governing equation for deformation can be obtained by substituting constitutive equation (equation (2)) into force balance equation:

$$\frac{\partial \sigma_{ij}}{\partial x_i} = 0 \quad (10)$$

and it becomes

$$\frac{3K(1-2\nu)}{2(1+\nu)} \nabla^2 u_i + \frac{3K}{2(1+\nu)} \frac{\partial \varepsilon}{\partial x_i} = \alpha \frac{\partial P}{\partial x_i} \quad (11)$$

where ν is drained Poisson's ratio, u_i is displacement for i^{th} direction, and ε is volumetric strain. To obtain equation (11) we use the relationships among the drained elastic parameters; that is,

$$G = \frac{3K(1-2\nu)}{2(1+\nu)} \quad (12)$$

2.2 Derivation of storage coefficients

In this section, we derive several storage coefficients for different mechanical boundary conditions and assumptions on the physical properties of constitutive materials. We also show that the three-dimensional storage coefficient (storage coefficient defined at constant mean normal stress) is the one that we measure during ordinary laboratory permeability experiments using a triaxial vessel.

(1) Constant mean normal stress

In this situation, the stress term on the right side of the equation (9) becomes 0 and the equation is treated as a homogeneous diffusion equation for fluid pressure. Here, the storage coefficient (S') becomes

$$S' = \rho_f g \left[\frac{1}{K} - \frac{1}{K_s} + \phi \left(\frac{1}{K_f} - \frac{1}{K_\phi} \right) \right] = \frac{\rho_f g \alpha}{KB} \quad (13)$$

Using the style of equation (1), S' is defined as

$$S' = g \left(\frac{dm_f}{dP} \right)_{\sigma_{kk}=0} \quad (14)$$

S' is named a three-dimensional storage coefficient (Kümpel, 1991).

Note that during the ordinary laboratory permeability experiments using a triaxial vessel, the mean applied stress is kept constant. Thus, the three-dimensional storage coefficient is the one we measure.

(2) Uniaxial strain and constant vertical stress

This condition is mathematically written as

$$\varepsilon_{11} = \varepsilon_{22} = 0, \sigma_{33} = 0 \quad (15)$$

This is usually assumed in the horizontal confined aquifer. Calculating ε_{11} and ε_{22} using equation (2) and summing them up yields

$$\frac{\sigma_{kk}}{3} = -\frac{4KG}{3K+4G} \left(\frac{1}{K} - \frac{1}{K_s} \right) P \quad (16)$$

This equation shows that the mean normal stress under this condition is proportional to the pore pressure. Substituting equation (16) into equation (9) gives

$$\kappa \nabla^2 P = \rho_f g \left[\left(\frac{1}{K} - \frac{1}{K_s} \right) \left(1 - \frac{4G \left(1 - \frac{K}{K_s} \right)}{3 \left(K + \frac{4G}{3} \right)} \right) + \phi \left(\frac{1}{K_f} - \frac{1}{K_\phi} \right) \right] \frac{\partial P}{\partial t} \quad (17)$$

Thus, the storage coefficient is defined as

$$S_s = \rho_f g \left[\left(\frac{1}{K} - \frac{1}{K_s} \right) \left(1 - \frac{4G \left(1 - \frac{K}{K_s} \right)}{3 \left(K + \frac{4G}{3} \right)} \right) + \phi \left(\frac{1}{K_f} - \frac{1}{K_\phi} \right) \right] \quad (18)$$

This storage coefficient is usually used in the field of hydrogeology and is termed the specific storage (Green and Wang, 1990). By comparing equations (13) and (18), the relationship between S' and S_s becomes

$$S_s = S' \left(1 - \frac{4GaB}{3K+4G} \right) \quad (19)$$

Using the style of equation (1), this storage coefficient (specific storage) can be defined as:

$$S_s = g \left(\frac{dm_f}{dP} \right)_{\epsilon_{11}=\epsilon_{22}=0, \sigma_{33}=0} \quad (20)$$

(3) Constant bulk volume

This situation is written as

$$\epsilon_{11} = \epsilon_{22} = \epsilon_{33} = 0 \quad (21)$$

It is also possible to define a storage coefficient (S_ϵ) for this particular situation. S_ϵ becomes

$$S_\epsilon = \rho_f g \left[\frac{K}{K_s} \left(\frac{1}{K} - \frac{1}{K_s} \right) + \phi \left(\frac{1}{K_f} - \frac{1}{K_\phi} \right) \right] \quad (22)$$

Comparing equations (13) and (22), we can get the relationship between S' and S_ϵ , and it is written as

$$S_\epsilon = S' - \rho_f g K \left(\frac{1}{K} - \frac{1}{K_s} \right)^2 = S' \frac{\rho_f g \alpha^2}{K} \quad (23)$$

Using equation (1), S_ϵ can be written as

$$S_\epsilon = g \left(\frac{dm_f}{dP} \right)_{\epsilon_{11}=\epsilon_{22}=\epsilon_{33}=0} \quad (24)$$

(4) Incompressible solid constituents

The assumption for incompressible solid constituents means $K/K_s \ll 1$ and $K/K_\phi \ll 1$. In this case, Biot-Willis parameter becomes unity. Thus, the three-dimensional storage coefficient and the specific storage become

$$S' = \rho_f g \left(\frac{1}{K} + \frac{\phi}{K_f} \right) \quad (25)$$

$$S_s = \rho_f g \left(\frac{1}{K_V} + \frac{\phi}{K_f} \right) \quad (26)$$

respectively. K_V in equation (26) is the drained bulk modulus under the uniaxial condition and is defined as

$$K_V = K + \frac{4G}{3} \quad (27)$$

In this situation, the condition for S_ϵ becomes the same as that for the condition of an undeformable porous framework. See subsection 2.2.(6) for a detailed definition of this coefficient. Equation (26) is the same as the specific storage defined by Jacob (1940) and Cooper (1966).

(5) Incompressible solid constituents and pore fluid

This situation assumes $K/K_s \ll 1$, $K/K_\phi \ll 1$, and $K/K_f \ll 1$. Here, equations (25) and (26) become

$$S' = \frac{\rho_f g}{K} \quad (28)$$

$$S_s = \frac{\rho_f g}{K_V} \quad (29)$$

Under this condition, Biot-Willis parameter and Skempton's B coefficient become unity. Note that the physical properties and the boundary conditions for equation (29) are the same as those for the Terzaghi consolidation.

(6) Undeformable porous framework

When the porous framework is not deformable, K ,

Table 1. Values of several different storage coefficients calculated from published data. Fluid density is assumed to be 1,000 kg/m³, and 9.8 m/s² is used for gravitational acceleration. To calculate storage coefficients with asterisks, bulk modulus for fluid is assumed to be 3.3 GPa for data from Detournay and Cheng (1993) and 2.3 GPa for data from Hart and Wang (1995).

Material	G (GPa)	K (GPa)	α	B	ϕ	S' (1/m)	S _s (1/m)	S _ε (1/m)	S'* (1/m)	S _s * (1/m)	S' (1/m)	S _s (1/m)	S* (1/m)	S (1/m)	Reference
Material properties									$K/K_s \ll 1$ $K/K_\phi \ll 1$		$K/K_s \ll 1$ $K/K_\phi \ll 1$ $K/K_f \ll 1$	$K \rightarrow \infty$ $K_s \rightarrow \infty$ $K_\phi \rightarrow \infty$	$K \rightarrow \infty$ $K_s \rightarrow \infty$ $K_f \rightarrow \infty$		
Ruhr sandstone	13	13	0.65	0.88	0.02	5.6E-7	3.8E-7	2.4E-7	8.1E-7	3.8E-7	7.5E-7	3.2E-7	5.9E-8	0	Detournay and Cheng (1993)
Tennessee marble	24	40	0.19	0.51	0.02	9.1E-8	8.7E-8	8.2E-8	3.0E-7	2.0E-7	2.5E-7	1.4E-7	5.9E-8	0	
Charcoal granite	19	35	0.27	0.55	0.02	1.4E-7	1.3E-7	1.2E-7	3.4E-7	2.2E-7	2.8E-7	1.6E-7	5.9E-8	0	
Berea sandstone	6.0	8.0	0.79	0.62	0.19	1.6E-6	1.2E-6	8.0E-7	1.8E-6	1.2E-6	1.2E-6	6.1E-7	5.6E-7	0	
Westerly granite	15	25	0.47	0.85	0.01	2.2E-7	1.8E-7	1.3E-7	4.2E-7	2.5E-7	3.9E-7	2.2E-7	3.0E-8	0	
Weber sandstone	12	13	0.64	0.73	0.06	6.6E-7	4.9E-7	3.5E-7	9.3E-7	5.2E-7	7.5E-7	3.4E-7	1.8E-7	0	
Ohio sandstone	6.8	8.4	0.74	0.50	0.19	1.7E-6	1.4E-6	1.1E-6	1.7E-6	1.1E-6	1.2E-6	5.6E-7	5.6E-7	0	
Pecos sandstone	5.9	6.7	0.83	0.61	0.20	2.0E-6	1.5E-6	9.8E-7	2.1E-6	1.3E-6	1.5E-6	6.7E-7	5.9E-7	0	
Boise sandstone	4.2	4.6	0.85	0.50	0.26	3.6E-6	2.8E-6	2.1E-6	2.9E-6	1.7E-6	2.1E-6	9.6E-7	7.7E-7	0	
Berea sandstone	5.6	6.6	0.77	0.75	0.19	1.5E-6	1.1E-6	6.4E-7	2.3E-6	1.5E-6	1.5E-6	7.0E-7	8.1E-7	0	
Indiana limestone	12	21	0.71	0.46	0.13	7.2E-7	6.2E-7	4.9E-7	1.0E-6	8.2E-7	4.7E-7	2.7E-7	5.5E-7	0	

K_s , and K_ϕ become infinity. In this situation, the storage coefficients become

$$S = S' = S_s = S_\varepsilon = \frac{\rho_f g \phi}{K_f} \quad (30)$$

(7) Undeformable porous framework and pore fluid

The storage coefficient becomes zero under this condition, and the fluid flow process in the porous media must be steady state.

Values of several different storage coefficients calculated from published data are shown in Table 1. The magnitudes of the different storage coefficients are in the following order:

$$S' \geq S_s \geq S_\varepsilon \quad (31)$$

S' is greatest because the least restraint is placed on the framework as fluid pressure is decreased. S_ε is smallest because the bulk volume is held constant, which means that the volume of fluid released is due primarily to fluid compressibility. It should be noted that S' and S_ε can be different more than two times for some rock samples (e.g., Ruhr sandstone, Berea sandstone, and Pecos sandstone). Considering that pore pressure decay is controlled by hydraulic diffusivity ($c = \kappa/S$), an accurate understanding of the concept of the storage coefficient and an appropriate choice of the coefficient for the problems considered are indispensable.

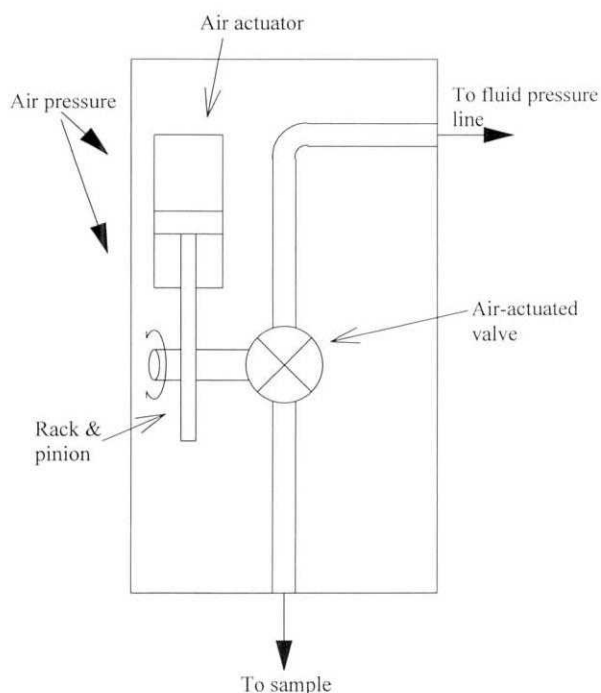


Fig. 1. Schematic figure of the newly developed endplug with built-in valve.

3. Experiments

3.1 Development of a new endplug

To accurately measure the physical properties of poroelastic materials, reducing the extra fluid volume in the measurement system is crucial. For example, Wissa (1969) suggested that the total volume of extra fluid in the system should be less than 3% of the pore volume in the test specimen. Here, we have developed a new endplug to accurately measure the physical properties and to easily control the fluid boundary condition.

The developed endplug (Figs. 1 and 2) contains a built-in plug, in which we applied a rack and pinion mechanism and activated it by an air actuator. The other (lower) endcap contained a pressure transducer and measured the pore pressure at the bottom of the sample (Fig. 3). The concept of the lower endcap is the same as that used by Green and Wang (1986) and Hart and Wang (1995). As a result, the extra fluid volume during the undrained experiments derives from the fluid between the built-in valve and the



Fig. 2. Photographs of the endplug used in this study.

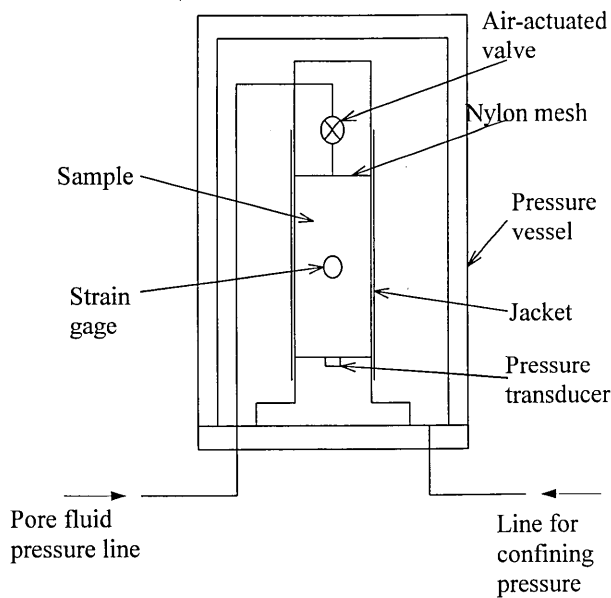


Fig. 3. Schematic figure of the experimental system.

sample top (about 0.1 cm^3) and that between the pressure transducer and the sample (about 0.06 cm^3), which is about 1% of the pore volume of the sample used in this experiment (about 15 cm^3). Thus, the physical properties measured with this system are treated as those for the tested sample without any problems. Also, changing the fluid boundary conditions (e.g., from undrained to drained conditions) is easily accomplished using the air actuator.

3.2 Sample description

The sample used in this experiment is Isahaya sandstone. Isahaya sandstone is of the Eocene age and has a porosity of about 8%. Isahaya sandstone has weak bedding planes and we cored samples perpendicular to the planes. The cored sample was 5.0 cm in diameter and 10 cm in height, and was saturated with degassed water.

3.3 Experimental procedure

Our experimental procedure was as follows:

1. Four strain gages were glued 90 degrees apart at the center of the sample (two for circumferential strains and two for axial strains), and the core side was sealed with silicone gel and a jacket.
2. Samples were submerged into degassed water under a vacuum for four to seven days to achieve saturation.
3. The sample was placed in a hydrostatic pressure vessel. A nylon mesh 0.2mm thick was inserted between the endplug containing the built-in valve

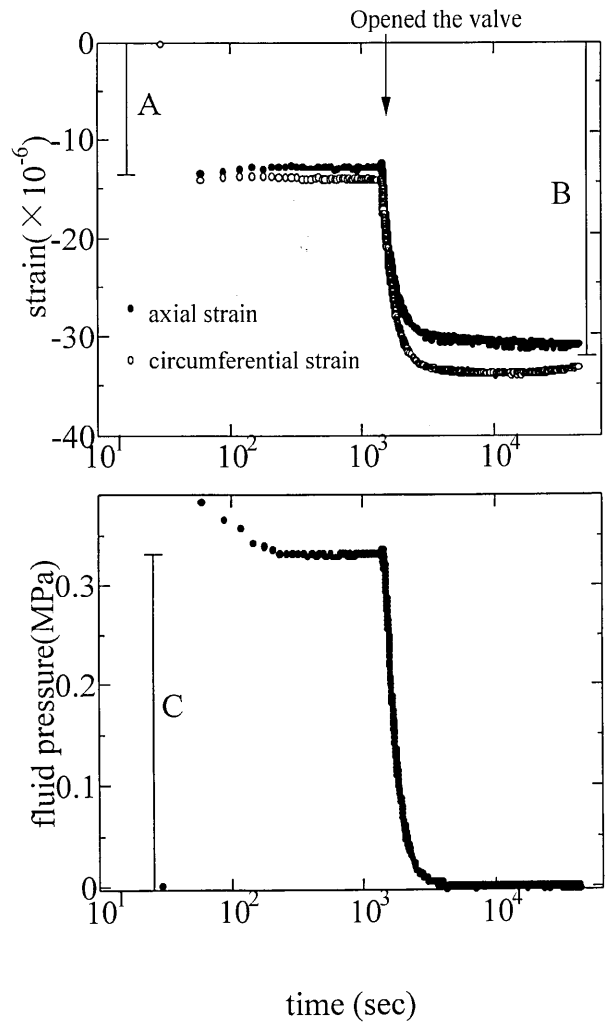


Fig. 4. Strains and fluid pressure data obtained. Note that extension is positive for strains.

and the sample to assure that the dewatering occurs through the whole upper surface of the sample.

4. The confining pressure was increased to 4.9 MPa, while the built-in valve was kept open for about three days. Then, the confining pressure was reduced to 4.4 MPa and kept constant for one day. During these stages, the pore fluid line pressure was kept at 0.78 MPa.
5. The built-in valve was closed and the confining pressure was increased to 4.9 MPa.
6. The built-in valve was opened, and strain and pore pressure changes were measured.
7. Similar experiments were conducted by changing the initial confining pressure to 3.9 MPa and 2.9 MPa (Table 2).

The triaxial vessel was placed in a room at a constant temperature to minimize the effects of tem-

A new method to determine hydraulic conductivity and storage coefficient through simultaneous measurements of fluid pressure and strains

perature fluctuations on pore pressure and strain measurements. Temperature fluctuations were less than 0.5 degrees Celcius during the experiments.

The data sets obtained from the experiment with the initial confining pressure at 4.4 MPa are shown in Fig. 4.

4. Evaluation of experimental data

Our experiments can be divided into three stages; i.e., undrained, pore pressure decay, and final steady (drained) state. The deformation at the first and third stages can be explained by undrained and drained poroelastic parameters, respectively. And, the second stage can also be explained by poroelastic parameters, as long as the sample behaves as a poroelastic medium.

We can get the undrained bulk modulus from the ratio between the strain during the undrained state (A in Fig. 4) and the increase of confining pressure (0.5 MPa), the drained bulk modulus from the ratio between the drained strain (B in Fig. 4) and the increase of confining pressure, and the Skempton's B coefficient from the ratio between pore pressure increase (C in Fig. 4) and the increase of confining pressure. Poroelastic parameters obtained from data sets shown in Fig. 4 appear in Table 2.

During the experiments, the circumferential strains are slightly larger than the axial strains. This difference may be due to anisotropy of the sample, however, the reason has not yet been clarified. In this analysis, the bulk moduli were calculated using the mean value of measured circumferential and axial strains.

Because only three independent parameters are necessary to explain the volumetric behavior of poroelastic material (Detournay and Cheng 1993), it is possible to calculate the storage coefficient using measured K , K_u , and B . By substituting equation (7) into equation (13), we can obtain

$$S' = \frac{\rho_f g}{KB^2} \left(1 - \frac{K}{K_u} \right) \quad (32)$$

The calculated three-dimensional storage coefficient

was 2.5×10^{-6} (1/m) (Table 2).

Transient pore pressure and strain behavior during the second stage can be explained by solving equations (6) and (11) simultaneously. To solve these equations, it is necessary to introduce a fourth parameter, ν (drained Poisson's ratio). The value of the Poisson's ratio must be between 0 and 0.5. Using the poroelastic properties obtained by our experiments and changing the drained Poisson's ratio (0.01 and 0.49), we calculated pore pressure and strains during pore pressure decay. Figure 5 shows the calculated

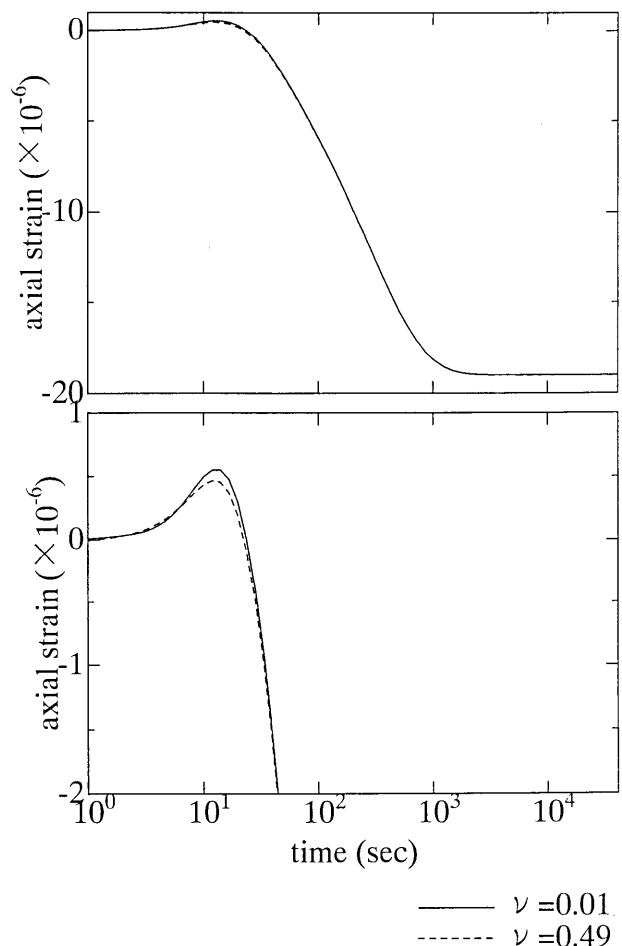


Fig. 5. Calculated axial strains during the pore pressure diffusion process. Note that the drained Poisson's ratio is not sensitive to strains.

Table 2. Parameters determined from this analysis. P_c indicates the initial confining pressure, ΔP_c the change of confining pressure, P_p the initial pore pressure.

K (GPa)	K_u (GPa)	B	S' (1/m)	κ (m/s)	P_c (MPa)	ΔP_c (MPa)	P_p (MPa)	Data
4.9	11.8	0.68	2.5×10^{-6}	3.5×10^{-11}	4.4	0.49	0.78	Figs. 4, 6, 7
4.5	12.9	0.71	2.8×10^{-6}	3.8×10^{-11}	3.9	0.49	0.78	Fig. 8a
3.7	13.6	0.81	2.9×10^{-6}	3.5×10^{-11}	2.9	0.49	0.78	Fig. 8b

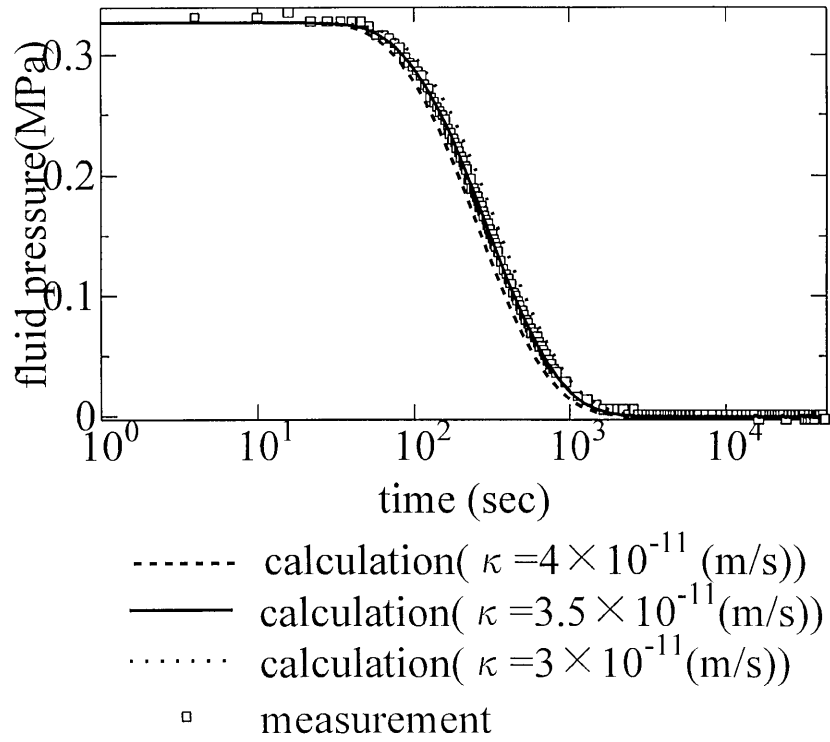


Fig. 6. Comparison of calculated and measured fluid pressures at the bottom of the sample.

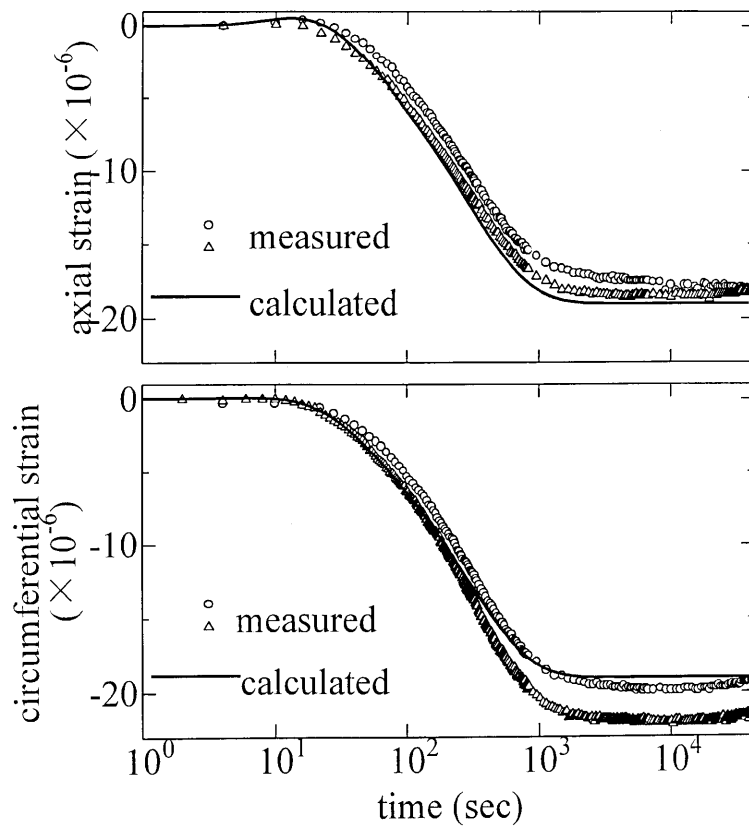


Fig. 7. Comparison of measured and calculated strain behavior. See text for details.

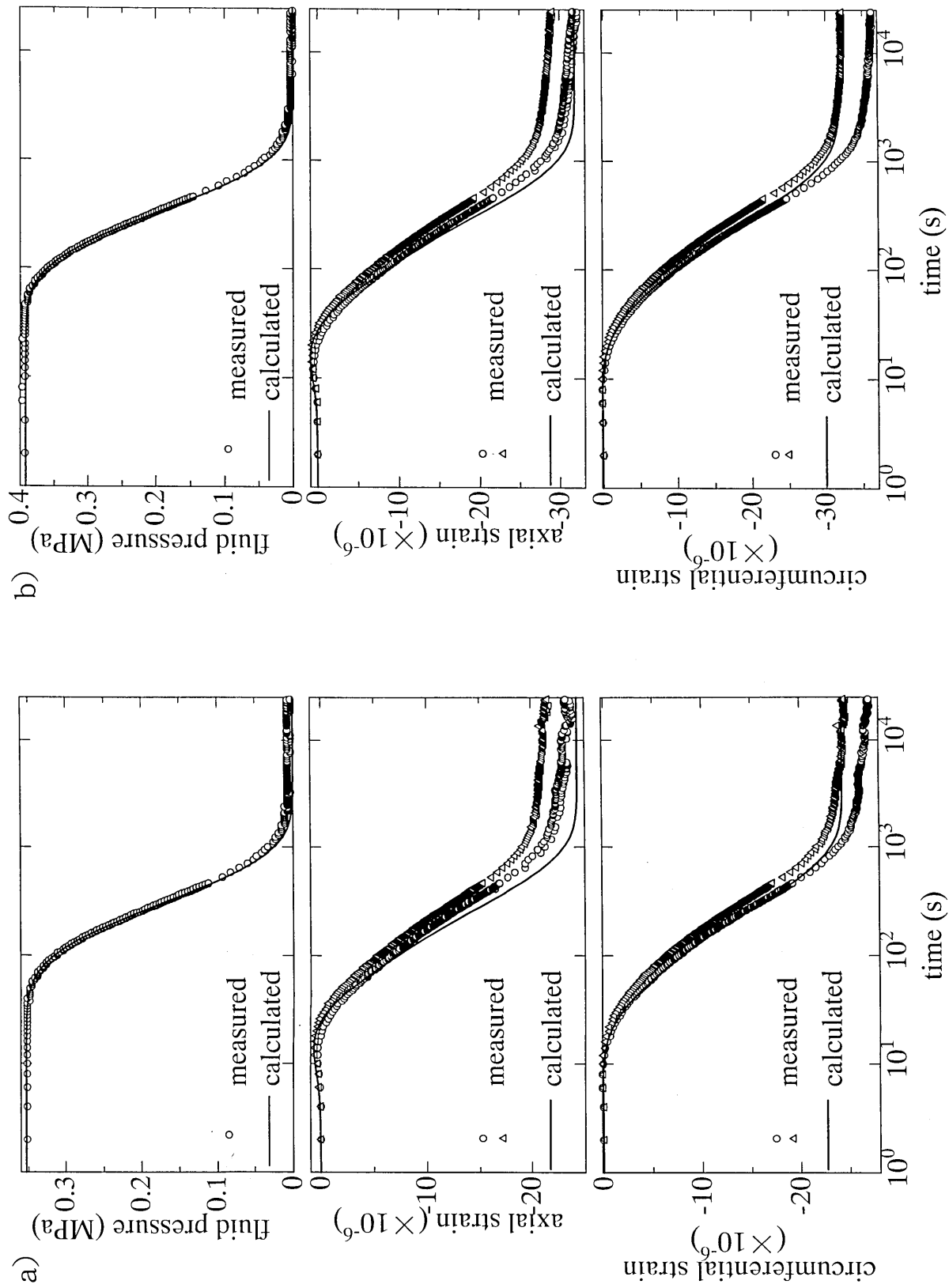


Fig. 8. Comparison between measured and calculated behavior of pore pressure and strains. Experimental condition and parameters used for the calculation are shown in Table 2.

axial strains. As shown in the figure, for the initial/boundary conditions applied in this particular experiment, the drained Poisson's ratio is not sensitive to the strains (and not relevant to pore pressure change). Aoyagi (2000) measured drained Poisson's ratio of Isahaya sandstone, and obtained the value 0.10. Thus, we assumed the drained Poisson's ratio of the sample to be 0.10.

Then, hydraulic conductivity is the only parameter necessary to describe strains and pore pressure during the second stage. Figure 6 is a comparison of measured and calculated pore pressure performance. The best-fit result for pore pressure decay was obtained when hydraulic conductivity was set at 3.5×10^{-11} (m/s) (Table 2).

Figure 7 shows a comparison between measured and calculated strain behavior at the center of the sample. Here, the transient extension of the axial strains at the early stage (about 10 seconds) and contraction afterwards were recognized both in measured and calculated results. Circumferential strains show monotonic contraction. This phenomenon is the same as that pointed out by Hart & Wang (1998); that is, by opening the built-in valve, the pore pressure at the top of the sample is reduced and the effective stress at the sample top is increased. The increase of the effective stress made the sample top contract, and the central part of the sample was forced to expand to keep the strain compatible. Then, as pore fluid pressure diffused through the sample, the center of the sample shrank due to the increase of the effective stress at that location.

Figure 8 shows a comparison between the experimental and calculated results under other initial confining pressure conditions. The measured strain behavior was reproduced well by the parameters in Table 2. Considering that the transient strain behavior was not used for determining the parameters, it can be said that the parameters obtained were reliable. In other words, the comparison between measured and calculated strain behavior during the second stage can be used to self-check the accuracy of the parameters obtained.

5. Conclusions

The concept of storage coefficient was discussed based on the theory of poroelasticity. It was shown that several storage coefficients can be defined by

different mechanical boundary conditions and assumptions on the physical properties of constitutive materials. It was also shown that three-dimensional storage coefficients were measured in most laboratory experiments, because we usually use triaxial and hydrostatic vessels. Calculations of several storage coefficients from published data suggest that an accurate understanding of the concept of the storage coefficient and the appropriate choice of coefficient for the problems considered are indispensable.

A new method to determine both hydraulic conductivity and storage coefficient through simultaneous measurements of fluid pressure and strains during experiments that were originally designed for measuring hydraulic conductivity was presented. We developed a new endplug to make it possible to reduce the extra volume of fluid in the measurement system (less than 1% of the pore fluid volume of the sample). Using the endplug, the storage coefficient was easily determined from direct measurements of poroelastic parameters. By analyzing the pore pressure diffusion process as a problem coupled to fluid flow and deformation, hydraulic conductivity was determined; and more importantly, a self-check of the accuracy of the parameters obtained became possible. This technique does not require complicated inversion calculations and can be used easily for parameter identification. Because hydraulic conductivity and storage coefficient are important parameters for modeling many geologic processes including the fluid movements and because there have not been much data on the storage coefficient, while accurately defining boundary conditions during measurements, the method developed in this paper helps to increase our understanding of the fluid flow process through geological formations.

Notation

- B: Skempton's B coefficient
- c: hydraulic diffusivity
- G: shear modulus
- g: gravitational acceleration
- h: hydraulic head
- K: drained bulk modulus
- K_f : bulk modulus of pore fluid
- K_s : unjacketed bulk modulus
- K_u : undrained bulk modulus
- K_V : drained bulk modulus under the uniaxial condi-

tion

- K_{ϕ} : reciprocal of the unjacketed pore compressibility
 m_f : fluid mass per unit bulk volume of porous material
 P : pore fluid pressure
 q_i : specific discharge
 S : storage coefficient (general)
 S' : storage coefficient at constant mean normal stress (three-dimensional storage coefficient)
 S_s : storage coefficient at uniaxial strain and constant vertical stress (specific storage)
 S_e : storage coefficient at constant bulk volume
 u_i : displacement
 α : Biot-Willis coefficient
 δ_{ij} : Kronecker's delta
 ϵ : volumetric strain
 ϵ_{ij} : bulk strain tensor of the representative elementary volume (REV) of a porous medium
 κ : hydraulic conductivity
 ν : drained Poisson's ratio
 ρ_f : pore fluid density
 σ_{ij} : total stress tensor on an REV
 ϕ : porosity

Acknowledgements

The authors would like to thank Kazunori Nishida and Akio Funato of OYO Corporation for their supports during the experimental study. The comments of Mitsuhiro Toriumi and an anonymous reviewer helped to improve the manuscript.

References

- Aoyagi, R., 2000MS., *Estimation of Physical Properties of Rock Masses Based on Poroelastic Theory*, MSc. Thesis, University of Tokyo, Tokyo, 138 pp.
 Berryman, J.G., 1992, Effective stress for transport properties of inhomogeneous porous rock. *J. Geophys. Res.*, **97**, 17409-17424.
 Biot, M.A., 1941, General theory of three-dimensional consolidation, *J. Appl. Phys.*, **12**, 155-164.
 Cooper, Jr., H.H., 1966, The equation of groundwater flow in fixed and deforming coordinates, *J. Geophys. Res.*, **84**, 7510-7512.
 Detournay, E. and A.H.-D. Cheng, 1993, Fundamentals of poroelasticity. In: J.A. Hudson (ed.), *Comprehensive Rock Engineering: Principles, Practice and Projects*. Oxford, Pergamon Press Vol. 2, 113-171.
 Esaki, T., M. Zhang, A. Takeshita and Y. Mitani, 1996, Rigorous theoretical analysis of a flow pump permeability test, *Geotech. Test. J.*, **19**, 241-246.
 Green, D.H. and H.F. Wang, 1986, Fluid pressure response to

- undrained compression in saturated sedimentary rock, *Geophys.*, **51**, 948-956.
 Green, D.H. and H.F. Wang, 1990, Specific storage as a poroelastic constant, *Water Resour. Res.*, **26**, 1631-1637.
 Hart, D.J. and H.F. Wang, 1995, Laboratory measurements of a complete set of poroelastic moduli for Berea sandstone and Indiana limestone, *J. Geophys. Res.*, **100**, 17741-17751.
 Hart, D.J. and H.F. Wang, 1998, Poroelastic effects during a laboratory transient pore pressure test, *Proc. Biot Conf. Poromechanics*, Rotterdam, Balkema, 579-582.
 Hart, D.J. and H.F. Wang, 2001, A single test method for determination of poroelastic constants and flow parameters in rocks with low hydraulic conductivities. *Int. J. Rock Mech. Min. Sci.*, **38**, 577-583.
 Jacob, C.E., 1940, On the flow of water in an elastic artesian aquifer, *EOS Trans., AGU*, **21**, 574-584.
 Kameya, H., N. Hirayama and A. Funato, 2001, Application of flow-pump permeability test method to low permeability rocks. *Proc. 31st Symp. Rock Mech. Japan*, Tokyo, 286-290. (in Japanese with English abstract)
 Kumpel, H.-J., 1991, Poroelasticity: Parameters reviewed, *Geophys. J. Int.*, **105**, 783-799.
 Narasimhan, T.N. and B.Y. Kanehiro, 1980, A note on the meaning of storage coefficient, *Water Resour. Res.*, **16**, 423-429.
 Neuzil, C.E., C. Cooley, S.E. Silliman, J.D. Bredehoeft and P.A. Hsieh, 1981, A transient laboratory method for determining the hydraulic properties of 'tight' rocks-II. Application, *Int. J. Rock Mech. Min. Sci. Geomech. Abstr.*, **18**, 253-258.
 Olsen, H.W., R.H. Morin and R.W. Nichols, 1988, Flow pump applications in triaxial testing. In: R.T. Donaghe, R.C. Chaney & M.L. Silver (eds.), *Advanced Triaxial Testing of Soil and Rock*, ASTM STP, **977**, 68-81.
 Rice, J.R. and M.P. Cleary, 1976, Some basic stress-diffusion solutions for fluid-saturated elastic porous media with compressible constituents, *Rev. Geophys. Space Phys.*, **14**, 227-241.
 Wang, H.F., 1993, Quasi-static poroelastic parameters in rock and their geophysical applications, *Pure Appl. Geophys.*, **141**, 269-286.
 Wang, H.F., 2000, *Theory of Linear Poroelasticity with Applications to Geomechanics and Hydrogeology*, Princeton, Princeton University Press, 287 pp.
 Wang, H.F. and D.J. Hart, 1993, Experimental error for permeability and specific storage from pulse decay measurements, *Int. J. Rock Mech. Min. Sci. Geomech. Abstr.*, **30**, 1173-1176.
 Wissa, A.E.Z., 1969, Pore pressure measurement in saturated stiff soils, *J. Soil Mech. Found. Div., Proc. Amer. Soc. Civil Eng.*, SM4, 1063-1073.
 Zhang, M., M. Takahashi, R.H. Morin, and T. Esaki, 2000, Evaluation and application of the transient-pulse technique for determining the hydraulic properties of low-permeability rocks-Part 2: Experimental application, *Geotech. Test. J.*, **23**, 91-99.

(Received June 23, 2001)

(Accepted December 7, 2001)